Published in final edited form as:
Genesis. 2010 January ; 48(1): 20–30. doi:10.1002/dvg.20578.

The zebrafish *dyrk1b* gene is important for endoderm formation

Gohar Mazmanian, **Michael Kovshilovsky**, **Debbie Yen**, **Aditya Mohanty**, **Sudipta Mohanty**, **Alex Nee**, and **Robert M. Nissen***
California State University Los Angeles, Department of Biological Sciences

Abstract

Nodal-signaling is required for specification of mesoderm, endoderm, establishing left-right asymmetry and craniofacial development. Wdr68 is a WD40-repeat domain-containing protein recently shown to be required for *endothelin-1 (edn1)* expression and subsequent lower jaw development. Previous reports detected the Wdr68 protein in multiprotein complexes containing mammalian members of the *dual-specificity tyrosine-regulated kinase (dyrk)* family. Here we describe the characterization of the zebrafish *dyrk1b* homolog. We report the detection of a physical interaction between Dyrk1b and Wdr68. We also found perturbations of Nodal signaling in *dyrk1b* antisense morpholino knockdown (*dyrk1b*-MO) animals. Specifically, we found reduced expression of *lft1* and *lft2* (*lft1/2)* during gastrulation and a near complete loss of the later asymmetric *lft1/2* expression domains. Although *wdr68*-MO animals did not display *lft1/2* expression defects during gastrulation, they displayed a near complete loss of the later asymmetric *lft1/2* expression domains. While expression of *ndr1* was not substantially effected during gastrulation, *ndr2* expression was moderately reduced in *dyrk1b*-MO animals. Analysis of additional downstream components of the Nodal signaling pathway in *dyrk1b*-MO animals revealed modestly expanded expression of the dorsal axial mesoderm marker *gsc* while the pan-mesodermal marker *bik* was largely unaffected. The endodermal markers *cas* and *sox17* were also moderately reduced in *dyrk1b*-MO animals. Notably, and similar to defects previously reported for *wdr68* mutant animals, we also found reduced expression of the pharyngeal pouch marker *edn1* in *dyrk1b*-MO animals. Taken together, these data reveal a role for *dyrk1b* in endoderm formation and craniofacial patterning in the zebrafish.

Keywords

Mirk; dyrk1b; wdr68; craniofacial; edn1

INTRODUCTION

Wdr68 is a WD40-repeat domain-containing protein originally identified as the vertebrate homolog of the petunia gene *AN11* (de Vetten *et al.*, 1997). *AN11* is required for production of the anthocyanin pigments in flower petals. The Wdr68 protein is also 45% similar to the arabidopsis TTG1 protein that is essential for proper specification of hair cell fates in the developing shoot and root (Schiefelbein, 2003; Walker *et al.*, 1999). More recently, the *wdr68* gene was identified in the zebrafish through an insertional mutagenesis screen as essential for development of the craniofacial apparatus (Amsterdam *et al.*, 2004; Nissen *et al.*, 2006). The *wdr68* gene is essential for both upper and lower jaw development in the zebrafish embryo. The *wdr68* gene is required upstream of the *endothelin-1 (edn1)* ligand that is in turn essential for the expression of several transcription factors including members

*Corresponding author: Robert M. Nissen, California State University Los Angeles, Department of Biological Sciences, 5151 State University Drive, Los Angeles, CA 90032, Phone (323)-343-2039, Fax (323-343-6451, rnissen@calstatela.edu.

of the *distal-less (dlx)* gene family that pattern the cranial neural crest giving rise to the lower jaw (Clouthier and Schilling, 2004; Miller *et al.*, 2000; Nissen *et al.*, 2006). Notably, *edn1* is not required for the embryonic upper jaw cartilage indicating that additional roles for *wdr68* beyond a requirement for *edn1* expression remain to be identified.

The mammalian Wdr68 protein has been detected in large multiprotein complexes containing two members of the *dual-specificity tyrosine-regulated kinase (dyrk)* family, Dyrk1a and Dyrk1b (Lim *et al.*, 2002; Skurat and Dietrich, 2004). Initial characterizations of human *DYRK1B/MIRK* revealed it to encode a nuclear localized protein enriched in skeletal muscle, testes, brain, heart and spleen with low levels of expression in most other tissues (Leder *et al.*, 2003; Leder *et al.*, 1999; Lee *et al.*, 2000). Several subsequent analyses showed Dyrk1b to be an important modulator of the G0-G1 cell cycle transition that is important for maintaining or achieving the differentiated state in several transformed cell lines (Deng *et al.*, 2009; Jin *et al.*, 2009). In the mouse myogenic C2C12 cell line, Dyrk1b inhibits association between Mef2d and the histone deacetylase MITR. This Dyrk1b-mediated differentiation switch is required for *myogenin* (*myog*) expression and subsequent myotube formation (Deng *et al.*, 2005; Deng *et al.*, 2003). In flies, a member of the *dyrk* family, *minibrain (mnb)*, is thought to play a role in cell proliferation because *mnb* mutant flies have fewer neurons in specific brain regions (Tejedor *et al.*, 1995). Similarly, a yeast homolog, yak1, is required for growth control and pseudohyphal differentiation (Garrett and Broach, 1989; Zhang *et al.*, 2001). Collectively, these data suggest a potential role for Dyrk1b-containing protein complexes in regulating cell differentiation events in vertebrates.

The Nodal-signaling pathway is required for specification of mesoderm, endoderm, establishing left-right asymmetry, and craniofacial development (Schier, 2003; Tian and Meng, 2006). During embryogenesis, the absence of Nodal signaling yields predominantly ectoderm, low levels of Nodal signaling are needed for mesoderm specification, and high levels are needed for endoderm specification (Gritsman *et al.*, 2000; Schier *et al.*, 1997; Thisse *et al.*, 2000). The Nodal-dependent transcription factors *casanova (cas)* and *sox17* are essential for endoderm specification (Alexander and Stainier, 1999; Dickmeis *et al.*, 2001; Kikuchi *et al.*, 2001). Later in development, signals emanating from the pharyngeal endoderm are important for craniofacial development (David *et al.*, 2002; Piotrowski and Nusslein-Volhard, 2000). The *endothelin-1 (edn1)* pathway is essential for lower jaw formation in several species (Crump *et al.*, 2004; Depew *et al.*, 2002; Kempf *et al.*, 1998; Kurihara *et al.*, 1994; Miller *et al.*, 2000; Nissen *et al.*, 2003). The small peptide ligand Edn1 is secreted by the pharyngeal pouch ectoderm and endoderm cells as well as by the arch core mesoderm. Edn1 signals through binding to a seven-transmembrane G protein-coupled receptor expressed on neural crest cells to regulate a downstream network of transcription factors important for lower jaw development (Clouthier *et al.*, 1998; Clouthier *et al.*, 2000; Ivey *et al.*, 2003). The *wdr68* gene is required for *edn1* expression in the zebrafish (Nissen *et al.*, 2006).

Although nuclear localization of both Wdr68 and a Dyrk1-family member was shown (Nissen *et al.*, 2006), a direct physical interaction between the zebrafish Wdr68 and Dyrk1b proteins has not been demonstrated. Likewise, the potential functional relationships between Wdr68 and Dyrk1b remain uncharacterized. To facilitate studies on the Dyrk1-Wdr68 complexes, we searched the zebrafish genome for genes homologous to the mammalian *dyrk1b* gene and identified a single zebrafish *dyrk1b* gene. Here, we report the detection of a physical interaction between zebrafish Dyrk1b and Wdr68, the expression pattern for *dyrk1b* during early development, and an initial characterization of *dyrk1b* antisense morpholino (*dyrk1b*-MO) knockdown animals.

RESULTS

Isolation of zebrafish *dyrk1b*

We performed BLAST searches on the zebrafish genome (Ensembl database assembly Zv8) to identify genes encoding proteins homologous to the human Dyrk1b protein. We found the putative zebrafish gene on chromosome 16. Using Clustal W to analyze sequence similarities, we found that it encodes a predicted protein that is 60% similar to human Dyrk1b and only 56% similar to human Dyrk1a (Thompson *et al.*, 1994). In accordance with Zebrafish nomenclature, we will from here forward refer to the chromosome 16 homolog as *dyrk1b*.

To characterize zebrafish *dyrk1b* further, we isolated cDNA fragments by performing 5′-RACE from cDNA of mixed zebrafish developmental stages using primers to the highly conserved kinase domain. Sequencing identified partial clones further confirming that the putative homolog is transcribed and spliced in embryos. Our sequencing-based assembled full-length sequence of *dyrk1b* was submitted to Genbank (GQ449256) and, notably, represents a 100% match to the independently predicted open reading frame contained in file XM_678964.

Zebrafish Dyrk1b and Wdr68 can physically interact

The mammalian Wdr68 and Dyrk1b proteins have been shown to physically interact in vitro (Skurat and Dietrich, 2004). To determine whether the zebrafish proteins might also form a physical complex, we tested them using an in vitro co-immunoprecipitation assay (Figure 1). We found that a FLAG-tagged zebrafish Wdr68 protein specifically co-immunoprecipitated the zebrafish Dyrk1b protein (Figure 1A, lane 5). Indicating specificity, we found that the FLAG-Wdr68 protein did not significantly co-immunoprecipitate a Luciferase control protein (Figure 1A, lane 4). Precipitated Dyrk1b protein was also not detected in the absence of the FLAG-Wdr68 protein ruling out a non-specific interaction between Dyrk1b and the FLAG antibody-bound protein-G sepharose beads (Figure 1A, lane 6). Substituting a negative control antibody for the FLAG antibody also resulted in the absence of any signal (Figure 1A, lanes 7–9). As additional negative controls, we found that neither p53 nor hoxb8a were capable of co-immunoprecipitating with FLAG-Wdr68 in our assay (Figure 1B). Since hoxb8a is similar in size to Flag-Wdr68, the experiments shown in Figure 1B were all conducted using non-radioactively labeled FLAG-Wdr68 protein that is therefore not detected in the autoradiographic image. Thus, we conclude that zebrafish Dyrk1b can physically interact with zebrafish Wdr68 in an in vitro assay.

dyrk1b is ubiquitously expressed during early development

To determine the expression pattern of *dyrk1b* we used the partial clone isolated by 5′-RACE to generate probes for use in whole-mount in situ hybridization (ISH). Expression of *dyrk1b* was detected ubiquitously by an antisense-strand probe from the earliest stage examined through to approximately the 10 somites stage (Figure 2A–F). The *dyrk1b* sense-strand probe served as the negative control (Figure 2B). Expression of *dyrk1b* was readily detected in the developing somites as well (Figure 2G–K). By 28hpf, *dyrk1b* expression in the head and pharyngeal arches region was significantly reduced relative to the level expressed in the somites (Figure 2J, K). The sense-strand probe served as the negative control at later stages as well (Figure 2I). Consistent with the ISH experiments, we also detected expression of *dyrk1b* by RT-PCR (Figure 3A). Notably, we detected maternal transcripts in the unfertilized oocyte cDNA sample (Figure 3A, lane 1). Since the primers used in the RT-PCR experiments are separated by several introns and over 8kb in the genome, the detected 636bp bands cannot represent amplification from genomic DNA. As controls for a known maternally supplied gene, we also found expression of *rpl35* in all

samples tested (Figure 3A). As negative control, *edn1* transcripts were not detected until after the tailbud stage (Figure 3A, lane 5).

Zebrafish *dyrk1b* is important for embryonic development

To determine what role the *dyrk1b* gene plays in zebrafish development, we created a gene knockdown model by designing a translation-blocking antisense morpholino oligonucleotide against the *dyrk1b* mRNA (*dyrk1b*-MO) as well as a 5-base mismatch control (control-MO). While animals injected with the control-MO appeared normal (Figure 3B), *dyrk1b*-MO animals displayed morphological defects including a smaller head and eyes as well as a moderately shortened body (Figure 3C). Animals injected with a second antisense morpholino against a *dyrk1b* intron-exon junction displayed a similar but milder phenotype (not shown). While survival of the control-MO animals did not differ from that of uninjected animals, the *dyrk1b*-MO animals rarely survived past 48hpf precluding analysis of later developmental stages or craniofacial cartilage formation.

Zebrafish *dyrk1b* and *wdr68* are important for *lft1* and *lft2* expression

The Nodal signaling antagonists, *lefty1 (lft1)* and *lefty2 (lft2)*, were originally identified as required for left-right asymmetry (Kosaki *et al.*, 1999; Meno *et al.*, 1997; Meno *et al.*, 1996). By morphological inspection of both *dyrk1b*-MO and *wdr68*-MO animals, we noted that the heart developed on the right side in many of the morphant animals instead of the left side, suggesting a defect in left-right asymmetry (data not shown). To explore the possibility of a left-right patterning defect further, we performed ISH analysis on *lft1* and *lft2* expression in *dyrk1b*-MO and *wdr68*-MO animals (Figure 4). Although initial expression of *lft1* prior to gastrulation appeared normal (Figure 4C, D), we found a subsequent failure to maintain both *lft1* and *lft2* expression during gastrulation in *dyrk1b*-MO animals (Figure 4E–H). Analyses of *lft1* and *lft2* expression in *wdr68*-MO animals did not reveal any substantial defects during gastrulation stages (data not shown). Expression of *fgf8* prior to gastrulation was also not significantly affected (Figure 4A, B). We also examined the later asymmetric expression of *lft1* and *lft2* after gastrulation (Figure 4I–P). At 18hpf, the asymmetric expression of *lft1* in the diencephalon was severely reduced in *wdr68*-MO animals (red arrows in Figure 4I, J, inset images). Expression of both *lft1* and *lft2* in the lateral plate mesoderm of the developing heart field was also severely reduced in *wdr68*-MO animals (black arrows in Figure 4I, J and K, L, respectively). We found similar losses in *dyrk1b*-MO animals (Figure 4M–P). At 20hpf in *dyrk1b*-MO animals, we found severely reduced expression of *lft1* in the diencephalon (red arrows in Figure 4M, N) and reduced expression of *lft2* in the lateral plate mesoderm of the developing heart field (black arrows in Figure 4O, P).

To test the specificity of the observed phenotypes, we injected control, *dyrk1b*-MO and *wdr68*-MO animals with in vitro transcribed RNA encoding EF1-alpha, Dyrk1b or FLAG-Wdr68 (Figure 4Q–T). We found that transcripts encoding Dyrk1b partially rescued the *lft2* expression defect in 40% of *dyrk1b*-MO animals (Figure 4R and Table 1). We also found that transcripts encoding FLAG-Wdr68 partially rescued the *lft2* expression defect in 43% of *wdr68*-MO animals (Figure 4T and Table 1). Notably, over-expression of Dyrk1b in wildtype animals disrupted *lft2* expression in 19% of animals injected while EF1-alpha over-expression had no substantial effect (Table 1).

dyrk1b is important for *ndr2* expression in zebrafish

While in mammals there is only one Nodal gene, in zebrafish there are three, *ndr1/sqt, ndr2/cyc,* and *spaw* (Long *et al.*, 2003; Rebagliati *et al.*, 1998a). Since the *ndr2* gene is predominantly responsible for mediating *lft1* and *lft2* expression (Feldman *et al.*, 2002), we examined the expression patterns of the zebrafish *nodal* genes (Figure 5). Expression of

ndr1 was not significantly reduced in *dyrk1b*-MO animals (Figure 5A, B). In contrast, expression of *ndr2* was significantly reduced at mid-gastrulation (Figure 5C, D) and later stages of gastrulation (Figure 5E, F). We also found severe reductions in the later asymmetric *ndr2* expression in the lateral plate mesoderm (black arrows in Figure 5G, H) and diencephalon of 20 somites stage *dyrk1b*-MO animals (red arrows in Figure 5G, H).

Since the asymmetric expression of both *ndr2* and the *lft1* and *lft2* genes are known to be dependent on *spaw* (Long *et al.*, 2003), we also examined the expression of *spaw*. We found loss of anterior *spaw* expression accompanied by symmetric posterior *spaw* expression in 20 somites stage *dyrk1b*-MO animals (black arrows in Figure 5I, J, are on left side of animals). In *wdr68*-MO animals, the milder phenotype of incorrect *spaw* expression on the right side of the animals was observed in 42% (10/24) of the animals examined compared to only 6% (3/46) of the control animals (black arrows in Figure 5K, L, are on the left side of animals).

dyrk1b is important for endoderm formation and *edn1* expression

While only moderate levels of Nodal signaling are needed for mesoderm specification, high levels are needed for endoderm specification (Gritsman *et al.*, 2000; Schier *et al.*, 1997; Thisse *et al.*, 2000). Therefore, we examined the expression of both mesoderm and endoderm markers in *dyrk1b*-MO animals (Figure 6). Expression of the pan-mesodermal marker *bik* was unaffected in *dyrk1b*-MO animals (Figure 6A, B). Likewise, expression of *flh* was not substantially affected (Figure 6C, D). Expression of the dorsal axial mesoderm marker *gsc* was modestly expanded in *dyrk1b*-MO animals (Figure 6E, F). In contrast, expression of the endoderm marker *cas* was significantly reduced during gastrulation in *dyrk1b*-MO animals (Figure 6G, H). Later expression of the *cas*-dependent endoderm marker *sox17* revealed reduced numbers of *sox17*-positive cells in *dyrk1b*-MO animals (Figure 6I, J).

The *wdr68* gene is required for expression of the *edn1* gene that, in turn, is required for lower jaw development in the zebrafish (Clouthier and Schilling, 2004; Miller *et al.*, 2000; Nissen *et al.*, 2006). Analysis of *edn1* expression revealed a significant reduction in the number of *edn1*-positive cells in *dyrk1b*-MO animals (compare regions underlined in red, Figure 6K, L).

DISCUSSION

Using 5′RACE and RT-PCR, we isolated transcripts representing a single zebrafish *dyrk1b* gene containing an open reading frame exactly matching an ORF independently proposed by an ORF prediction algorithm. In mammals, *dyrk1b* is subject to alternative splicing and an alternative exon1 has been identified in mice (Leder *et al.*, 2003). Nonetheless, our 5′-RACE experiments using primers in the *dyrk1b* kinase domain failed to detect an alternative 5′-exon variant in the zebrafish. Since the experiments presented here focused on early developmental stages, further analyses that extend into adult stages might reveal the existence of an alternative exon1 in zebrafish.

Consistent with previous results using the mammalian proteins (Skurat and Dietrich, 2004), we found that the zebrafish Dyrk1b protein was capable of engaging in a specific physical interaction with Wdr68 (Figure 1). In tissue culture cells, Wdr68 localizes to the nucleus (Nissen *et al.*, 2006). Several reports indicate that Dyrk1b can also localize to the nucleus (Deng *et al.*, 2004; Leder *et al.*, 1999; Lee *et al.*, 2000). Taken together, these data suggest that a nuclear Wdr68-Dyrk1b protein complex may exist.

Our analysis revealed the near ubiquitous expression of *dyrk1b* during early development in the zebrafish with enrichment in the developing somites at later stages (Figure 2).

Expression of *dyrk1b* in the developing somites is consistent with the reported role for *dyrk1b* in muscle differentiation (Deng *et al.*, 2003). In C2C12 cells, *dyrk1b* is required for *myogenin* expression and inhibits association between Mef2d and the histone deacetylase MITR revealing a role as a transcriptional co-regulator (Deng *et al.*, 2005;Deng *et al.*, 2003). Coupled with the Wdr68 interaction assay results, we speculate that a Wdr68-Dyrk1b transcriptional co-regulator complex may exist in the zebrafish.

Several of our results reveal that *dyrk1b* and *wdr68* share common regulatory targets (Figure 4, 5, 6). We found that both *dyrk1b* and *wdr68* are required for the asymmetric expression of *lft1* and *lft2* (Figure 4). Similarly, both genes are important for normal asymmetric expression of *spaw* (Figure 5). Likewise, both *dyrk1b* and *wdr68* are important for *edn1* expression (Figure 6)(Nissen *et al.*, 2006). We also found that *dyrk1b* is important for *ndr2, cas, sox17, lft1* and *lft2* expression during gastrulation stages. However, we did not find significant defects in *ndr2, cas, sox17, lft1* or *lft2* expression during gastrulation stages in *wdr68*-MO animals (data not shown). While it is possible that *dyrk1b* and *wdr68* function independently in the regulation of these target genes, we speculate that the loss of the catalytic Dyrk1b subunit of the Wdr68-Dyrk1b complex might be more detrimental to overall complex function than the loss of the Wdr68 subunit, for which a biochemical activity remains unknown. Consistently, the *spaw* expression defect was less severe in *wdr68*-MO animals than in *dyrk1b*-MO animals (Figure 5).

During embryogenesis, low levels of Nodal signaling specify mesoderm while high levels specify endoderm (Gritsman *et al.*, 2000; Schier *et al.*, 1997; Thisse *et al.*, 2000). We found that *ndr2* expression was reduced, but not lost, in *dyrk1b*-MO animals (Figure 5C–F). We also found a modest expansion of the expression of the dorsal axial mesoderm marker *gsc* in *dyrk1b*-MO animals (Figure 6E–F). At similar developmental stages we also found reduced expression of the endoderm markers *cas* and *sox17* in *dyrk1b*-MO animals (Figure 6G–J). These results are consistent with the current model for Nodal signaling in which high levels of signal are needed for endoderm induction while only low levels are needed for mesoderm induction. Notably, the zebrafish phenotype for complete loss of *ndr2* activity is cyclopia (Rebagliati *et al.*, 1998b), a phenotype we never observed in *dyrk1b*-MO animals. The absence of cyclopia in *dyrk1b*-MO animals is consistent with our observed moderate reduction, but not loss, of *ndr2* expression.

The *wdr68* gene is important for craniofacial development in the zebrafish (Nissen *et al.*, 2006). We previously found that *wdr68* is essential for expression of the lower jaw patterning gene *edn1* (Clouthier and Schilling, 2004; Miller *et al.*, 2000; Nissen *et al.*, 2006). Here, we found that *dyrk1b* is also important for *edn1* expression suggesting a role for *dyrk1b* in craniofacial development in the zebrafish (Figure 6K–L).

A mouse knockout of *dyrk1b* was made but unfortunately lost before a detailed characterization of the mutant animals could be completed (Leder *et al.*, 2003). Although it is unlikely that defects fully comparable to those described here for the zebrafish were present but overlooked in the mutant mice, the unavailability of the mutant mouse line precludes a definitive assessment. Regardless, a possible explanation for any phenotypic discrepancies suspected between the mouse and fish, based on the preliminary characterization of the now lost mouse mutant, may lie in the evolutionary differences in the Nodal signaling pathway between the two organisms. Namely, zebrafish have 3 nodal-related genes while mice appear to only have one. The evolutionary split of the single mammalian nodal gene functions amongst multiple teleost nodal-related genes might also have been accompanied by neomorphic changes in gene regulatory roles for various other loci such as *dyrk1b* and/or *wdr68*. Recreation of a *dyrk1b* mutant mouse line will be needed to fully explore these possibilities.

Taken together, these results suggest that a Wdr68-Dyrk1b complex may mediate some of the roles previously observed for *wdr68* in the zebrafish. Future studies will be needed to further explore the roles of this complex.

MATERIALS AND METHODS

Animal husbandry

Wildtype TAB5 and TAB14 zebrafish strains were maintained essentially as described (Nissen *et al.*, 2006).

5′-RACE, PCR subcloning and RT-PCR

RACE was performed using the SMART RACE kit (Clontech) as previously described (Golling *et al.*, 2002). 5′-RACE fragments were subcloned into pCR-bluntII vectors (Invitrogen) for sequencing. The 5′-RACE primers were dyrk1b-r1 5′-TTGTAGGAGAGAAGCTCAAACACCAG-3′ and dyrk1b-r2 5′-AGGCACAGGTGGTTACGGAACAT-3′. The 5′-RACE fragment was subcloned into a pCRbluntII vector yielding the plasmid pCRbluntII-dyrk1b-5′R. To clone full-length *dyrk1b*, the following additional primers were used: dyrk1b-start 5′-ATGTCGAGCCAGCACAGCCAC-3′, dyrk1b-stop 5′-TCAAGAGTTGGCTGCACTCTGACC-3′, dyrk1b-sub1 5′-ttcttcggatccgatatcgcgaattccaccATGTCGAGCCAGCACAGC-3′, dyrk1b-sub2 5′-ttcttcctcgagTCAAGAGTTGGCTGCACTCTG-3′. A full-length ORF clone was inserted into a pCRbluntII vector yielding the plasmid pCRbluntII-dyrk1b-2256. The plasmid pCS2+dyrk1b-2256 was generated by subcloning the EcoRI fragment from plasmid pCRbluntII-dyrk1b-2256 into the vector pCS2+. For stage-specific RT-PCR analysis of *dyrk1b* expression, total RNA was isolated from specific developmental stages and used for 1st strand synthesis as previously described (Nissen *et al.*, 2006). The primers used to detect *dyrk1b* transcripts are dyrk1b-kin-f1 5′-GTGGCCATCAAGATCATCAAGAACAAG-3′ and dyrk1b-kin-r1 5′-GGTCGAAGTATTTGCGTGCTTTAGG-3′. The primers for *rpL35* were previously described (Nissen *et al.*, 2006).

Co-immunoprecipitation assay

The FLAG-tagged zebrafish Wdr68 construct was previously described (Nissen *et al.*, 2006). Translation-grade 35S-methionine was purchased from GE Healthcare. Co-immunoprecipitation assays were performed using a TNT Quick-Coupled Transcription-Translation Kit as per the manufacturer recommendations (Promega, catalog # L2080). The pCS2+Dyrk1b-2256 plasmid was used to generate full-length zebrafish Dyrk1b and the pCS2+FLAG-Wdr68 plasmid was used to generate FLAG-Wdr68 protein. The plasmid for generating the luciferase control protein was provided in the TNT kit. The plasmid for generating the zebrafish p53 control protein was kindly provided by Dr. Kirsten Edepli. The plasmid for generating the zebrafish hoxb8a control protein was previous described (Mansfield *et al.*, 2004). Briefly, after pre-blocking protein-G sepharose beads (Invitrogen, catalog # 10-1242) with 1uL reticulocyte lysate per 100uL packed beads, we washed the beads with Wash buffer (50mM Tris pH 7.8; 250mM NaCl; 0.1% Triton X-100; 1% BSA; 1mM β-mercaptoethanol) three times. To create immunocomplexes, 4uL of each translated 35S-labeled protein to be tested was mixed in a 25uL total volume of Wash buffer containing 1uL of FLAG-Antibody (Rockland catalog # NC9120608) and incubated at 4°C for 1 hour. The reaction was then centrifuged for 5 minutes at 13,000 rpm and the supernatant transferred to 30μl of a 50% slurry of the blocked protein-G sepharose beads and mixed at 4°C for 1 hour with mild agitation. After capturing the immunocomplexes, the beads were washed 3 times with 1.5mL Wash buffer to remove unbound material followed by two additional washes with Wash buffer lacking the BSA. Bound complexes were eluted

from the beads in SDS-PAGE Buffer and ran on an SDS-PAGE gel. The gel was dried, exposed to autoradiographic film overnight, developed and scanned into a digital image. All co-immunoprecipitation experiments were performed at least twice.

Antisense morpholinos used in this study

The translation blocking morpholino sequence used in this study for the *dyrk1b* gene was dyrk1b-3 5′-gtgctggctcgacatggttggctca-3′ and the sequence complementary to the start codon is underlined. A second morpholino sequence dyrk1b-4 5′-CCTCTTTAAGTGGActgaggagaca-3′ designed against a *dyrk1b* splicing junction was also used and the upper case sequence corresponds to the exon sequence while lowercase corresponds to the intron sequence. The 5-base mismatch control morpholino sequence for the translation blocking morpholino used in this study is dyrk1b-5mis 5′-gtgctggctcCaGatgCttgCctGa-3′ and the capital letters indicate the mismatch changes. The morpholino against *wdr68* was previously described (Nissen *et al.*, 2006). Wildtype embryos were free-hand injected at the 1–4 cell stages with approximately 1–4nL of a solution containing 200uM morpholino using pulled glass needles and a picospritzer as previously described (Nissen *et al.*, 2003). A hemacytometer was used to calibrate needles and quantify volumes injected into animals.

Whole-mount in situ hybridization (WISH) analysis

WISH was performed as previously described (Nissen *et al.*, 2003). The plasmid pCRbluntII-dyrk1b-5′R was digested with SpeI and transcribed with T7 to generate an approximately 1.5kb antisense probe against *dyrk1b*. The plasmid pCRbluntII-dyrk1b-5′R was digested with EcoRV and transcribed with SP6 to generate an approximately 1.5kb control sense probe for the same region of *dyrk1b* as that targeted by the antisense probe. The *lft1* and *lft2* probes were synthesized from DNA fragments generated by RT-PCR with the following primer pairs: Lft1-F1 5′-ctcctgcaccttgaaaagATGACT-3′, Lft1-R1 5′-CTTTCTGAGGTTCCACCCAGTAGA-3′, Lft1-t7R1 5′-TAATACGACTCACTATAGGGCTTTCTGAGGTTCCACCCAGTAGA-3′, Lft2-F1 5′-CTGTTCATCCAGCTGTTCATTTTG-3′, Lft2-R1 5′-ACTTCGGTGTTTTCCTGAAGTCTG-3′, Lft2-t7R1 5′-TAATACGACTCACTATAGGGACTTCGGTGTTTTCCTGAAGTCTG-3′. The *cas* probe was synthesized from DNA fragments generated by RT-PCR with the following primer pairs: cas-f1 5′-ATGTATCTCGACCGGATGCTCC-3′ and cas-t7r1 5′-TAATACGACTCACTATAGGgcagcaatctggatggaagc-3′. The *sox17* probe was synthesized from DNA fragments generated by RT-PCR with the following primer pairs: sox17-f1 5′-gatgagcgcaagaggcttgc-3′ and sox17-t7r1 5′-TAATACGACTCACTATAGGgctcaaactccacctcgtcc-3′. The *flh* probe was synthesized from DNA fragments generated by RT-PCR with the following primer pairs: flh-f1 5′-ctaaacagacgccatgcagattcc-3′ and flh-t7r1 5′-TAATACGACTCACTATAGGgactcttctgtgaaatccctctcc-3′. The plasmids for generating probes to detect the *ndr1*, *ndr2* (Rebagliati *et al.*, 1998b), *spaw* (Long *et al.*, 2003), *fgf8* (Reifers *et al.*, 1998), *gsc* (Schulte-Merker *et al.*, 1994), *bik* (Chen and Schier, 2002) and *edn1* (Miller *et al.*, 2000) transcripts were previously described. All in situ hybridizations described were repeated at least twice and representative images were selected for inclusion in all figures.

In vitro transcription and mRNA injections

The plasmids pCS2+dyrk1b-2256 and pCS2+FLAG-Wdr68 were digested with NotI and used for in vitro transcription using the SP6 mMessage mMachine kit as per the manufacturers recommendations (Ambion, catalog # AM1340). The EF1-alpha control plasmid was supplied in the kit. After spin column purification and quantification,

approximately 1–4nL of a 200ng/uL solution was injected into embryos at the 1–4 cell stage either alone or in combinations with antisense morpholinos described earlier. Embryos were harvested at the 20 somites stage and processed for in situ hybridization. The data presented in Table 1 represent the combined results from two independent experiments.

Acknowledgments

Contract grant sponsor: National Science Foundation IOS-0744454

We thank Jenny Arvizu for providing excellent management of the Cal State LA zebrafish colony. This work was supported by a grant from CSUPERB and grant #IOS-0744454 from the National Science Foundation.

References

Alexander J, Stainier DY. A molecular pathway leading to endoderm formation in zebrafish. Curr Biol. 1999; 9:1147–1157. [PubMed: 10531029]

Amsterdam A, Nissen RM, Sun Z, Swindell EC, Farrington S, Hopkins N. Identification of 315 genes essential for early zebrafish development. Proc Natl Acad Sci U S A. 2004; 101:12792–12797. [PubMed: 15256591]

Chen Y, Schier AF. Lefty proteins are long-range inhibitors of squint-mediated nodal signaling. Curr Biol. 2002; 12:2124–2128. [PubMed: 12498687]

Clouthier DE, Hosoda K, Richardson JA, Williams SC, Yanagisawa H, Kuwaki T, Kumada M, Hammer RE, Yanagisawa M. Cranial and cardiac neural crest defects in endothelin-A receptor-deficient mice. Development. 1998; 125:813–824. [PubMed: 9449664]

Clouthier DE, Schilling TF. Understanding endothelin-1 function during craniofacial development in the mouse and zebrafish. Birth Defects Res C Embryo Today. 2004; 72:190–199. [PubMed: 15269892]

Clouthier DE, Williams SC, Yanagisawa H, Wieduwilt M, Richardson JA, Yanagisawa M. Signaling pathways crucial for craniofacial development revealed by endothelin-A receptor-deficient mice. Dev Biol. 2000; 217:10–24. [PubMed: 10625532]

Crump JG, Swartz ME, Kimmel CB. An integrin-dependent role of pouch endoderm in hyoid cartilage development. PLoS Biol. 2004; 2:E244. [PubMed: 15269787]

David NB, Saint-Etienne L, Tsang M, Schilling TF, Rosa FM. Requirement for endoderm and FGF3 in ventral head skeleton formation. Development. 2002; 129:4457–4468. [PubMed: 12223404]

de Vetten N, Quattrocchio F, Mol J, Koes R. The an11 locus controlling flower pigmentation in petunia encodes a novel WD-repeat protein conserved in yeast, plants, and animals. Genes Dev. 1997; 11:1422–1434. [PubMed: 9192870]

Deng X, Ewton DZ, Friedman E. Mirk/Dyrk1B maintains the viability of quiescent pancreatic cancer cells by reducing levels of reactive oxygen species. Cancer Res. 2009; 69:3317–3324. [PubMed: 19351855]

Deng X, Ewton DZ, Mercer SE, Friedman E. Mirk/dyrk1B decreases the nuclear accumulation of class II histone deacetylases during skeletal muscle differentiation. J Biol Chem. 2005; 280:4894–4905. [PubMed: 15546868]

Deng X, Ewton DZ, Pawlikowski B, Maimone M, Friedman E. Mirk/dyrk1B is a Rho-induced kinase active in skeletal muscle differentiation. J Biol Chem. 2003; 278:41347–41354. [PubMed: 12902328]

Deng X, Mercer SE, Shah S, Ewton DZ, Friedman E. The cyclin-dependent kinase inhibitor p27Kip1 is stabilized in G(0) by Mirk/dyrk1B kinase. J Biol Chem. 2004; 279:22498–22504. [PubMed: 15010468]

Depew MJ, Lufkin T, Rubenstein JL. Specification of jaw subdivisions by Dlx genes. Science. 2002; 298:381–385. [PubMed: 12193642]

Dickmeis T, Mourrain P, Saint-Etienne L, Fischer N, Aanstad P, Clark M, Strahle U, Rosa F. A crucial component of the endoderm formation pathway, CASANOVA, is encoded by a novel sox-related gene. Genes Dev. 2001; 15:1487–1492. [PubMed: 11410529]

Feldman B, Concha ML, Saude L, Parsons MJ, Adams RJ, Wilson SW, Stemple DL. Lefty antagonism of Squint is essential for normal gastrulation. Curr Biol. 2002; 12:2129–2135. [PubMed: 12498688]

Garrett S, Broach J. Loss of Ras activity in Saccharomyces cerevisiae is suppressed by disruptions of a new kinase gene, YAKI, whose product may act downstream of the cAMP-dependent protein kinase. Genes Dev. 1989; 3:1336–1348. [PubMed: 2558053]

Golling G, Amsterdam A, Sun Z, Antonelli M, Maldonado E, Chen W, Burgess S, Haldi M, Artzt K, Farrington S, Lin SY, Nissen RM, Hopkins N. Insertional mutagenesis in zebrafish rapidly identifies genes essential for early vertebrate development. Nat Genet. 2002; 31:135–140. [PubMed: 12006978]

Gritsman K, Talbot WS, Schier AF. Nodal signaling patterns the organizer. Development. 2000; 127:921–932. [PubMed: 10662632]

Ivey K, Tyson B, Ukidwe P, McFadden DG, Levi G, Olson EN, Srivastava D, Wilkie TM. Galphaq and Galpha11 proteins mediate endothelin–1 signaling in neural crest-derived pharyngeal arch mesenchyme. Dev Biol. 2003; 255:230–237. [PubMed: 12648486]

Jin K, Ewton DZ, Park S, Hu J, Friedman E. Mirk regulates the exit of colon cancer cells from quiescence. J Biol Chem. 2009

Kempf H, Linares C, Corvol P, Gasc JM. Pharmacological inactivation of the endothelin type A receptor in the early chick embryo: a model of mispatterning of the branchial arch derivatives. Development. 1998; 125:4931–4941. [PubMed: 9811577]

Kikuchi Y, Agathon A, Alexander J, Thisse C, Waldron S, Yelon D, Thisse B, Stainier DY. casanova encodes a novel Sox-related protein necessary and sufficient for early endoderm formation in zebrafish. Genes Dev. 2001; 15:1493–1505. [PubMed: 11410530]

Kosaki K, Bassi MT, Kosaki R, Lewin M, Belmont J, Schauer G, Casey B. Characterization and mutation analysis of human LEFTY A and LEFTY B, homologues of murine genes implicated in left-right axis development. Am J Hum Genet. 1999; 64:712–721. [PubMed: 10053005]

Kurihara Y, Kurihara H, Suzuki H, Kodama T, Maemura K, Nagai R, Oda H, Kuwaki T, Cao WH, Kamada N, et al. Elevated blood pressure and craniofacial abnormalities in mice deficient in endothelin-1. Nature. 1994; 368:703–710. [PubMed: 8152482]

Leder S, Czajkowska H, Maenz B, De Graaf K, Barthel A, Joost HG, Becker W. Alternative splicing variants of dual specificity tyrosine phosphorylated and regulated kinase 1B exhibit distinct patterns of expression and functional properties. Biochem J. 2003; 372:881–888. [PubMed: 12633499]

Leder S, Weber Y, Altafaj X, Estivill X, Joost HG, Becker W. Cloning and characterization of DYRK1B, a novel member of the DYRK family of protein kinases. Biochem Biophys Res Commun. 1999; 254:474–479. [PubMed: 9918863]

Lee K, Deng X, Friedman E. Mirk protein kinase is a mitogen-activated protein kinase substrate that mediates survival of colon cancer cells. Cancer Res. 2000; 60:3631–3637. [PubMed: 10910078]

Lim S, Zou Y, Friedman E. The transcriptional activator Mirk/Dyrk1B is sequestered by p38alpha/beta MAP kinase. J Biol Chem. 2002; 277:49438–49445. [PubMed: 12384504]

Long S, Ahmad N, Rebagliati M. The zebrafish nodal-related gene southpaw is required for visceral and diencephalic left-right asymmetry. Development. 2003; 130:2303–2316. [PubMed: 12702646]

Mansfield JH, Harfe BD, Nissen R, Obenauer J, Srineel J, Chaudhuri A, Farzan-Kashani R, Zuker M, Pasquinelli AE, Ruvkun G, Sharp PA, Tabin CJ, McManus MT. MicroRNA-responsive ‘sensor’ transgenes uncover Hox-like and other developmentally regulated patterns of vertebrate microRNA expression. Nat Genet. 2004; 36:1079–1083. [PubMed: 15361871]

Meno C, Ito Y, Saijoh Y, Matsuda Y, Tashiro K, Kuhara S, Hamada H. Two closely-related left-right asymmetrically expressed genes, lefty-1 and lefty-2: their distinct expression domains, chromosomal linkage and direct neuralizing activity in Xenopus embryos. Genes Cells. 1997; 2:513–524. [PubMed: 9348041]

Meno C, Saijoh Y, Fujii H, Ikeda M, Yokoyama T, Yokoyama M, Toyoda Y, Hamada H. Left-right asymmetric expression of the TGF beta-family member lefty in mouse embryos. Nature. 1996; 381:151–155. [PubMed: 8610011]

Miller CT, Schilling TF, Lee K, Parker J, Kimmel CB. sucker encodes a zebrafish Endothelin-1 required for ventral pharyngeal arch development. Development. 2000; 127:3815–3828. [PubMed: 10934026]

Nissen RM, Amsterdam A, Hopkins N. A zebrafish screen for craniofacial mutants identifies wdr68 as a highly conserved gene required for Endothelin-1 expression. BMC Dev Biol. 2006; 6:28. [PubMed: 16759393]

Nissen RM, Yan J, Amsterdam A, Hopkins N, Burgess SM. Zebrafish foxi one modulates cellular responses to Fgf signaling required for the integrity of ear and jaw patterning. Development. 2003; 130:2543–2554. [PubMed: 12702667]

Piotrowski T, Nusslein-Volhard C. The endoderm plays an important role in patterning the segmented pharyngeal region in zebrafish (Danio rerio). Dev Biol. 2000; 225:339–56. [PubMed: 10985854]

Rebagliati MR, Toyama R, Fricke C, Haffter P, Dawid IB. Zebrafish nodal-related genes are implicated in axial patterning and establishing left-right asymmetry. Dev Biol. 1998a; 199:261–272. [PubMed: 9698446]

Rebagliati MR, Toyama R, Haffter P, Dawid IB. cyclops encodes a nodal-related factor involved in midline signaling. Proc Natl Acad Sci U S A. 1998b; 95:9932–9937. [PubMed: 9707578]

Reifers F, Bohli H, Walsh EC, Crossley PH, Stainier DY, Brand M. Fgf8 is mutated in zebrafish acerebellar (ace) mutants and is required for maintenance of midbrain-hindbrain boundary development and somitogenesis. Development. 1998; 125:2381–2395. [PubMed: 9609821]

Schiefelbein J. Cell-fate specification in the epidermis: a common patterning mechanism in the root and shoot. Curr Opin Plant Biol. 2003; 6:74–78. [PubMed: 12495754]

Schier AF. Nodal signaling in vertebrate development. Annu Rev Cell Dev Biol. 2003; 19:589–621. [PubMed: 14570583]

Schier AF, Neuhauss SC, Helde KA, Talbot WS, Driever W. The one-eyed pinhead gene functions in mesoderm and endoderm formation in zebrafish and interacts with no tail. Development. 1997; 124:327–342. [PubMed: 9053309]

Schulte-Merker S, Hammerschmidt M, Beuchle D, Cho KW, De Robertis EM, Nusslein-Volhard C. Expression of zebrafish goosecoid and no tail gene products in wild- type and mutant no tail embryos. Development. 1994; 120:843–852. [PubMed: 7600961]

Skurat AV, Dietrich AD. Phosphorylation of Ser640 in muscle glycogen synthase by DYRK family protein kinases. J Biol Chem. 2004; 279:2490–2498. [PubMed: 14593110]

Tejedor F, Zhu XR, Kaltenbach E, Ackermann A, Baumann A, Canal I, Heisenberg M, Fischbach KF, Pongs O. minibrain: a new protein kinase family involved in postembryonic neurogenesis in Drosophila. Neuron. 1995; 14:287–301. [PubMed: 7857639]

Thisse B, Wright CV, Thisse C. Activin- and Nodal-related factors control antero-posterior patterning of the zebrafish embryo. Nature. 2000; 403:425–428. [PubMed: 10667793]

Thompson JD, Higgins DG, Gibson TJ. CLUSTAL W: improving the sensitivity of progressive multiple sequence alignment through sequence weighting, position-specific gap penalties and weight matrix choice. Nucleic Acids Res. 1994; 22:4673–4680. [PubMed: 7984417]

Tian T, Meng AM. Nodal signals pattern vertebrate embryos. Cell Mol Life Sci. 2006; 63:672–685. [PubMed: 16465442]

Walker AR, Davison PA, Bolognesi-Winfield AC, James CM, Srinivasan N, Blundell TL, Esch JJ, Marks MD, Gray JC. The TRANSPARENT TESTA GLABRA1 locus, which regulates trichome differentiation and anthocyanin biosynthesis in Arabidopsis, encodes a WD40 repeat protein. Plant Cell. 1999; 11:1337–1350. [PubMed: 10402433]

Zhang Z, Smith MM, Mymryk JS. Interaction of the E1A oncoprotein with Yak1p, a novel regulator of yeast pseudohyphal differentiation, and related mammalian kinases. Mol Biol Cell. 2001; 12:699–710. [PubMed: 11251081]

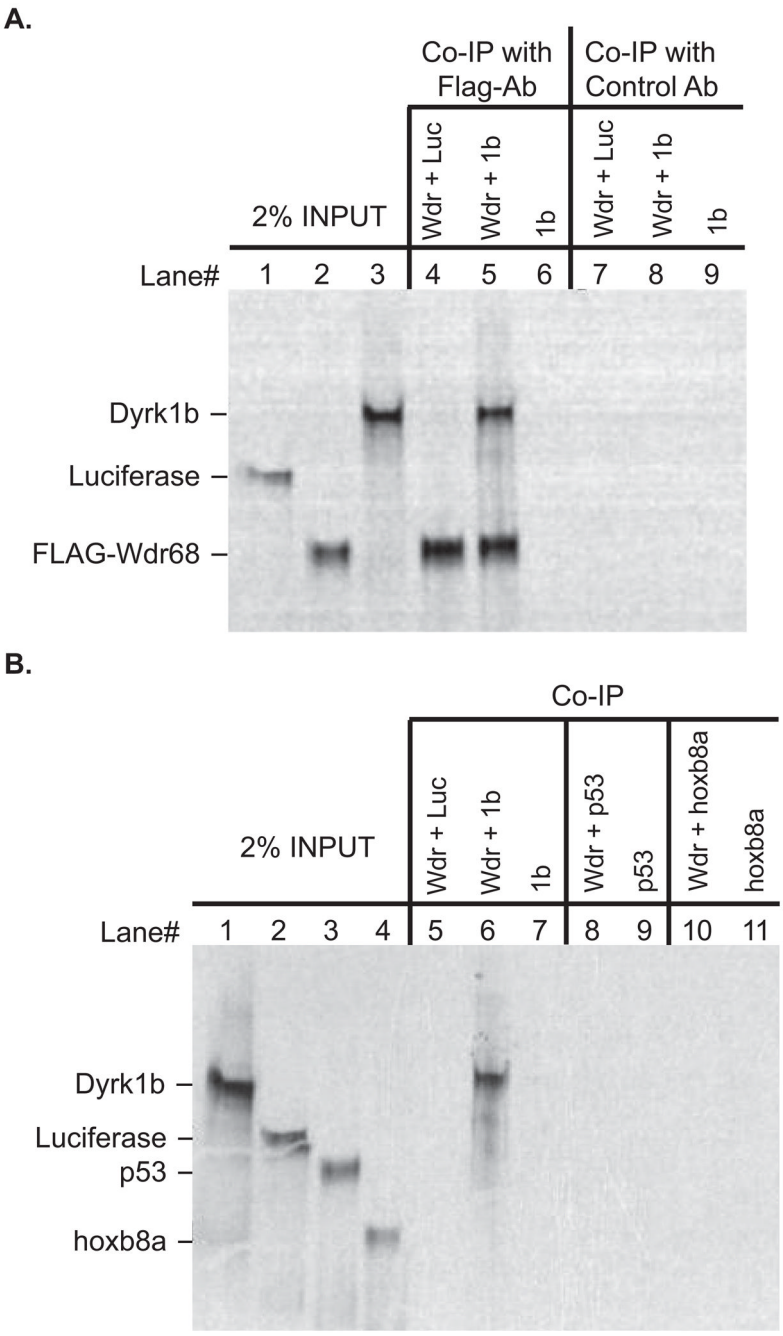

Figure 1. The zebrafish Wdr68 and Dyrk1b proteins can physically interact

A) Lane 1 shows 2% of the negative control Luciferase protein input. Lane 2 shows 2% of the FLAG-Wdr68 protein input. Lane 3 shows 2% of the Dyrk1b protein input. Lane 4 shows the results of a co-immunoprecipitation (co-IP) between FLAG-Wdr68 and Luciferase indicating no co-IP of the negative control Luciferase. Lane 5 shows the results of a co-IP between FLAG-Wdr68 and Dyrk1b indicating that Dyrk1b can physically interact with FLAG-Wdr68. Lane 6 shows the dependence of the Dyrk1b co-IP on the presence of FLAG-Wdr68. Lanes 7–9 are the same as lanes 4–6 but with the FLAG antibody substituted with an unrelated histone H3 control antibody. B) Lane 1 shows 2% of Dyrk1b input. Lane 2 shows 2% of negative control Luciferase input. Lane 3 shows 2% of negative control p53

input. Lane 4 shows 2% of negative control hoxb8a input. The FLAG-Wdr68 protein used in these experiments was translated with non-radioactive amino acids and is therefore not detected in the image. Lane 5 shows the results of a co-IP between FLAG-Wdr68 and Luciferase indicating no co-IP of the negative control Luciferase. Lane 6 shows the results of a co-IP between FLAG-Wdr68 and Dyrk1b indicating that Dyrk1b can physically interact with FLAG-Wdr68. Lane 7 shows the dependence of the Dyrk1b co-IP on the presence of FLAG-Wdr68. Lanes 8–9 show the lack of interaction between FLAG-Wdr68 and the negative control p53. Lanes 10–11 show the lack of interaction between FLAG-Wdr68 and the negative control hoxb8a.

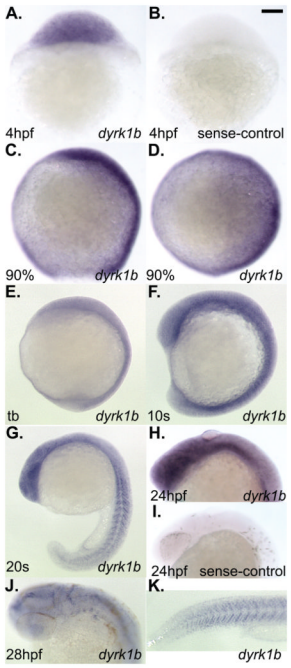

Figure 2. Whole-mount in situ hybridization analysis of *dyrk1b* expression in wildtype zebrafish embryos

A) ubiquitous expression of *dyrk1b* at 4hpf. B) sense-strand negative control for staining also at 4hpf. C) lateral view of 90% epiboly stage, D) dorsal view of 90% epiboly stage. E) lateral view of tailbud (tb) stage. F) lateral views of 10 somites (10s) stage. G) lateral view of 20 somites (20s) stage. H) lateral view of 24hpf stage. I) sense-strand negative control for staining also at 24hpf. J) dorsolateral view of 28hpf stage. K) lateral tail view of the same animal shown in panel J. Scale bar in panel B = 100 micrometers length.

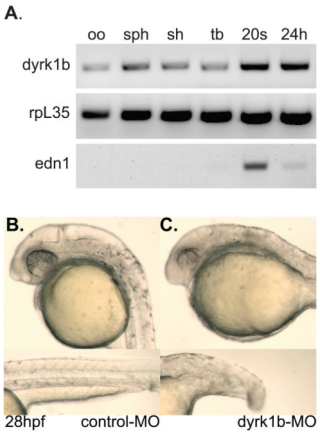

Figure 3. *dyrk1b* is maternally supplied and essential during embryonic development in the zebrafish

A) RT-PCR detection of *dyrk1b* transcripts in unfertilized oocytes (oo), sphere stage (sph), shield stage (sh), tailbud stage (tb), 20 somites stage (20s), and 24 hours post fertilization (24h) stage animals. The *rpl35* gene serves as positive control. The *edn1* gene serves as negative control for detection in oocytes. B) Normal phenotype of 5-mismatch control morpholino-injected (control-MO) animals at 28hpf. Upper panel shows normal head, eye, pigment and ear development. Lower panel shows normal notochord, tail and somite development. C) Phenotype of *dyrk1b* antisense morpholino-injected (*dyrk1b*-MO) animals at 28hpf. Upper panel shows small head and eyes of the morphant animals. Lower panel shows the moderately shortened length of the tail.

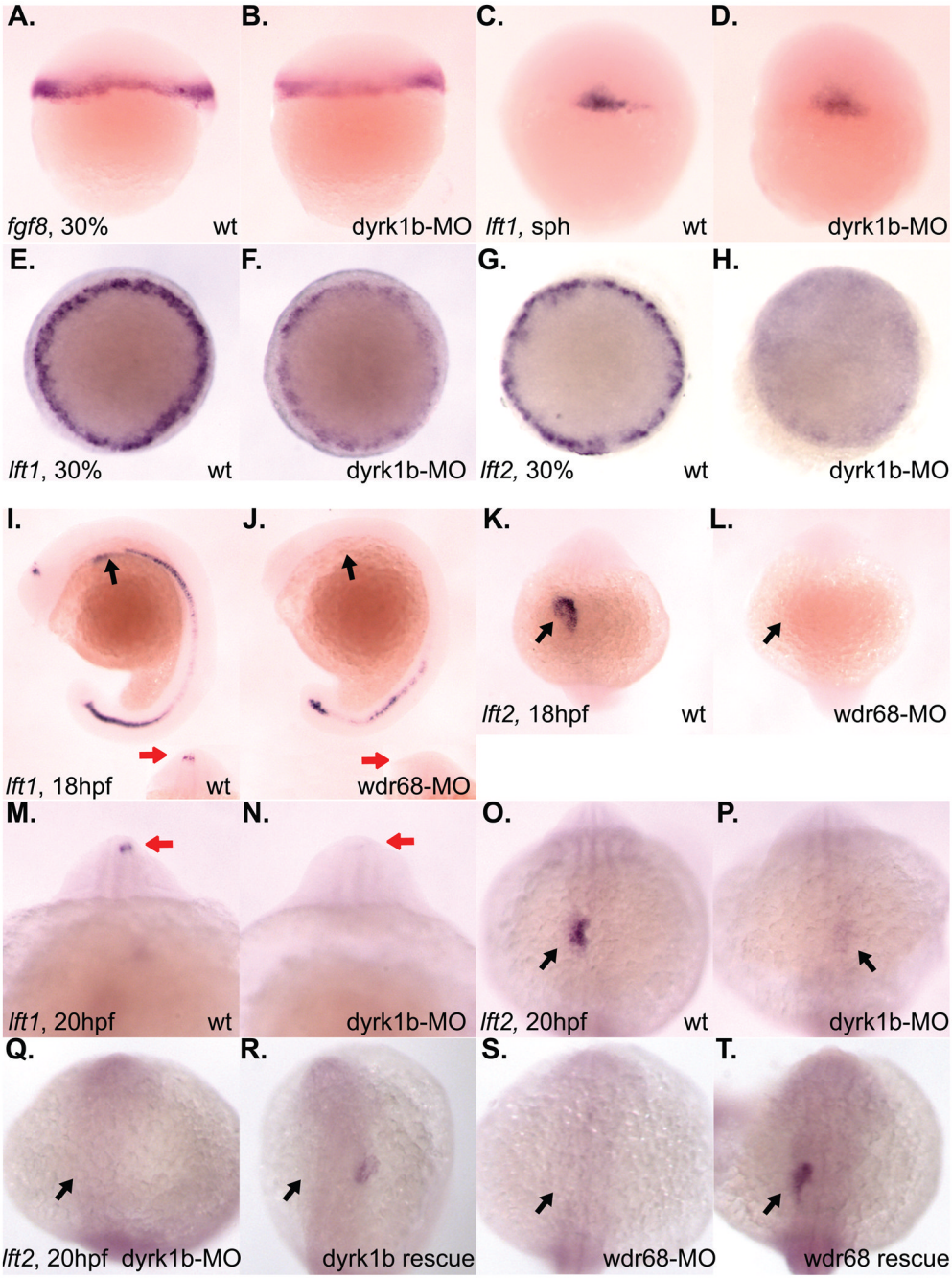

Figure 4. Reduced expression of *lft1* and *lft2* in *dyrk1b* and *wdr68* knockdown animals

A) lateral view of normal *fgf8* expression in control animals at 30% epiboly stage. B) normal *fgf8* expression in *dyrk1b*-MO animals at 30% epiboly stage. C) lateral view of normal *lft1* expression in control animals at sphere (sph) stage. D) normal *lft1* expression in *dyrk1b*-MO animals at sphere stage. E) dorsal view of normal *lft1* expression in control animals at 30% epiboly stage. F) reduced *lft1* expression in *dyrk1b*-MO animals at 30% epiboly stage. G) dorsal view of normal *lft2* expression in control animals at 30% epiboly stage. H) reduced *lft2* expression in *dyrk1b*-MO animals at 30% epiboly stage. I) lateral view of normal *lft1* expression in control animals at 18hfp. Black arrows indicate asymmetric expression in the lateral plate mesoderm of the developing heart field. Red arrows in inset images are on the

left side of the animals and indicate asymmetric expression in the diencephalon. J) severely reduced *lft1* expression in the asymmetric heart and diencephalon territories of *wdr68*-MO animals at 18hpf. K) dorsal view of normal *lft2* expression in control animals at 18hpf. Black arrows indicate asymmetric expression in the lateral plate mesoderm of the developing heart field. L) severely reduced *lft2* expression in the asymmetric heart and diencephalon territories of *wdr68*-MO animals at 18hpf. M) anterior view of normal *lft1* expression in the asymmetric diencephalon territory of control animals at 20hpf. Red arrows are on the left side of the animals and indicate asymmetric expression in the diencephalon. N) severely reduced *lft1* expression in the asymmetric diencephalon territory of *dyrk1b*-MO animals at 20hpf. O) dorsal view of normal *lft2* expression in the asymmetric heart territory of control animals at 20hpf. Black arrows indicate asymmetric expression in the lateral plate mesoderm of the developing heart field. P) severely reduced *lft2* expression in the asymmetric heart territory of *dyrk1b*-MO animals at 20hpf. Q) dorsal view of severely reduced *lft2* expression in *dyrk1b*-MO animals co-injected with EF1alpha transcripts. R) partial rescue of *lft2* expression in *dyrk1b*-MO animals co-injected with Dyrk1b transcripts. S) dorsal view of severely reduced *lft2* expression in *wdr68*-MO animals co-injected with EF1alpha transcripts. T) partial rescue of *lft2* expression in *wdr68*-MO animals co-injected with FLAG-Wdr68 transcripts.

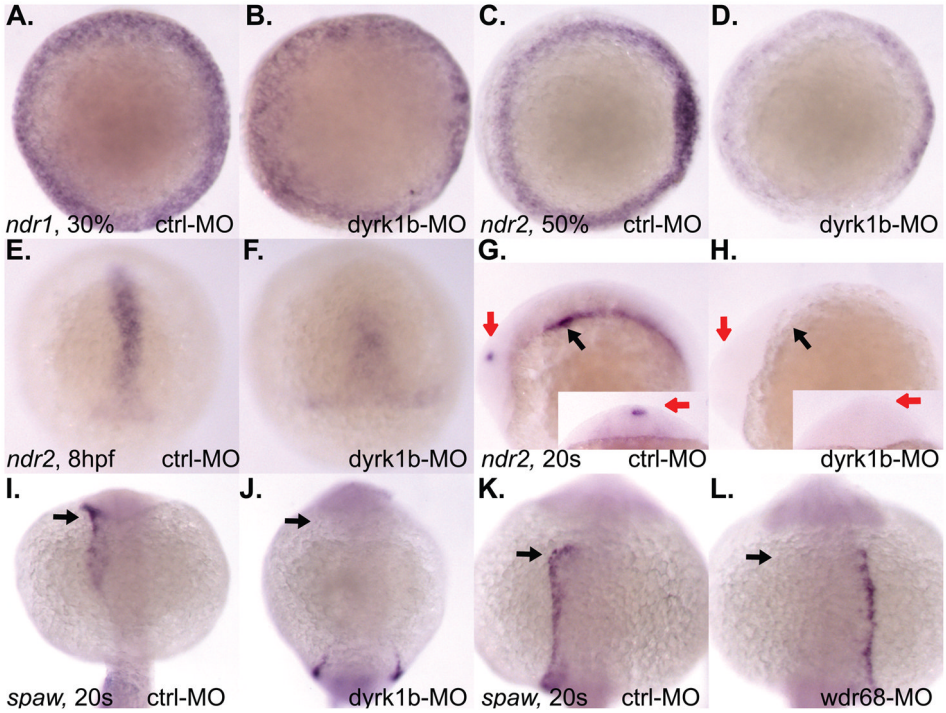

Figure 5. *dyrk1b* and *wdr68* are important for *ndr2* and *spaw* expression in the zebrafish

A) dorsal view of normal *ndr1* expression in control animals at 30% epiboly stage. B) normal *ndr1* expression in *dyrk1b*-MO animals at 30% epiboly stage. C) A) normal *ndr2* expression in control animals at 50% epiboly stage. D) reduced *ndr2* expression in *dyrk1b*-MO animals at 50% epiboly stage. E) shield view of normal *ndr2* expression in control animals at 8hpf. F) reduced *ndr2* expression in *dyrk1b*-MO animals at 8hpf. G) normal asymmetric *ndr2* expression in control animals at 20 somites stage. Black arrow indicates asymmetric expression in lateral plate mesoderm. Red arrows indicate asymmetric expression in diencephalon. Red arrow in inset image is on left side of animal. H) reduced *ndr2* expression in *dyrk1b*-MO animals at 20 somites stage. I) dorso-posterior view of normal asymmetric *spaw* expression in control animals at 20 somites stage. J) reduced expression of *spaw* in *dyrk1b*-MO animals at 20 somites stage. K) dorsal view of normal asymmetric *spaw* expression in control animals at 20 somites stage. L) loss of asymmetry in the expression of *spaw* in *wdr68*-MO animals at 20 somites stage.

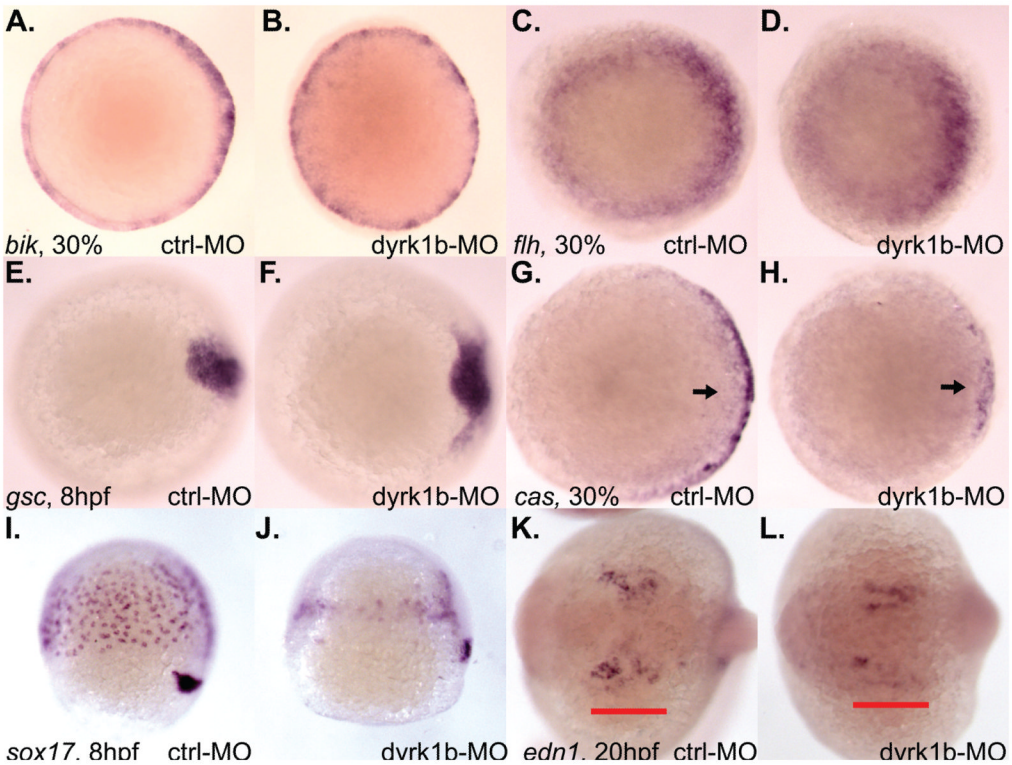

Figure 6. *dyrk1b* is important for endoderm induction and *edn1* expression in the zebrafish

A) normal *bik* expression in control animals at 30% epiboly stage. B) normal *bik* expression in *dyrk1b*-MO animals at 30% epiboly stage. C) normal *flh* expression in control animals at 30% epiboly stage. D) normal *flh* expression in *dyrk1b*-MO animals at 30% epiboly stage. E) normal *gsc* expression in control animals at 8hpf. F) modest expansion of *gsc* expression in *dyrk1b*-MO animals at 8hpf. G) normal *cas* expression in control animals at 30% epiboly stage. H) reduced *cas* expression in *dyrk1b*-MO animals at 30% epiboly stage. I) normal *sox17* expression in control animals at 8hpf. J) reduced *sox17* expression in *dyrk1b*-MO animals at 8hpf. K) normal *edn1* expression in control animals at 20hpf. Red bar underlines pharyngeal expression domain of *edn1*. L) reduced *edn1* expression in *dyrk1b*-MO animals at 20hpf.

Table 1

Partial RNA rescue of *lft2* expression defects

MO and transcript injected	***lft2* detected**	***lft2* not detected**
Control-MO + EF1alpha	107 (98%)	2 (2*%)
dyrk1b-MO + EF1alpha	20 (19%)	83 (81%)
dyrk1b-MO + Dyrk1b	25 (40%)	38 (60%)
wdr68-MO + EF1alpha	7 (16%)	37 (84%)
wdr68-MO + FLAG-Wdr68	24 (43%)	32 (57%)
EF1alpha	31 (100%)	0 (0%)
Dyrk1b	62 (81%)	15 (19%)